Large variations in the onset of rippling in concentric nanotubes

H. Jackman,[1, a)] P. Krakhmalev,[1] and K. Svensson[1]
Department of Engineering and Physics, Karlstad University, SE-651 88 Karlstad, Sweden

(Dated: 22 November 2013)

We present a detailed experimental study of the onset of rippling in highly crystalline carbon nanotubes. Modeling has shown that there should be a material constant, called the critical length, describing the dependence of the critical strain on the nanotube outer radius. Surprisingly, we have found very large variations, by a factor of three, in the critical length. We attribute this to a supporting effect from the inner walls in multiwalled concentric nanotubes. We provide an analytical expression for the maximum deflection prior to rippling, which is an important design consideration in nanoelectromechanical systems utilizing nanotubes.

Nanotubes can now be made in a variety of materials, such as carbon, boron nitride and metal-disulfides. These materials have a high mechanical stiffness that is promising for future nanoscale devices, such as relays[1,2] and resonators.[3,4] During bending the tubes can however deform in buckling or rippling patterns, much like macroscopic tubes do, and the bending stiffness will drop significantly. Such deformations have been observed for nanotubes made of C,[5,6] BN,[7,8] and WS_2,[9] while similar deformations are also expected to occur in MoS_2.[10]

The rippling deformations will reduce the bending stiffness by a factor of two or more.[11–15] In a relay configuration this would result in a lower switching frequency and quality factor, or even a bi-stable operation due to stiction. Although stiction is a common problem in nanorelays,[16] the influence of rippling on the performance is often neglected when analyzing a relay.[17] The rippling can also influence the strength of fibre composites as it reduces the reinforcing effect.[18] While the appearance of rippling in nanotubes is well known to occur, less is known about when the rippling will commence and how it depends on the size and internal structure of the tubes. Theoretical modeling of the rippling onset in carbon nanotubes (CNTs) suggests that the critical strain ε_{cr} is inversely proportional to the nanotube outer radius.[13–15,19] From this dependence one can define a material constant, $l_{cr} = \varepsilon_{cr} r_o$, which has the dimension of a length and is referred to as the critical length. The theoretical studies have however found rather different values for this critical length. This diversity could come from differences in the models or an actual variation in the critical length, dependent on the nanotube geometry. The critical length sets an upper limit on the linear, high bending stiffness, range as the maximum deflection is directly proportional to l_{cr}.[20] Thereby, the critical length is an important factor in applications where the high bending stiffness of nanotubes are exploited.

As the atomic rearrangement is very small at the very onset of buckling and rippling,[14] the onset is best detected in force-displacement curves by the sudden drop in stiffness, and has only recently been measured experimentally.[12] While the measurements have revealed values of the critical strain that are comparable to those from theoretical modeling, it also demonstrated a strong influence from structural defects in the tubes (grown by chemical vapor deposition (CVD)). A detailed comparison with theoretical modeling could therefore not be made in that study.

In this letter we present measurements of the onset for rippling in multiwalled carbon nanotubes (MWCNTs) of high crystallinity (grown by arc-discharge). The high crystallinity enables a detailed study of the critical strain and critical length, without any influence from structural defects in the nanotubes. We have found values of the critical strain that are comparable to previous modeling. However, unexpectedly large variations in the critical length (about a factor of three) were observed. The critical length displays a strong dependence on the internal structure of the nanotubes and it should not be thought of as a material constant.

In order to measure the critical strain (ε_{cr}) the free end of individual cantilevered CNTs were deflected inside a transmission electron microscope (TEM), using a commercial AFM-TEM instrument from Nanofactory Instruments AB. Arc-discharge grown CNTs, obtained from professor Hui-Ming Cheng,[21] was dispersed in dichloroethane and then sonicated for 15 minutes. This dispersion was then drop-casted onto a glass substrate, leaving well separated particles that could be attached to the tip of a silver wire using conductive epoxy glue. The silver wire was mounted on a tip holder that sits on a sapphire ball attached to a piezoelectric tube, see Fig. 1 (a). A piezoresistive force sensor was located opposite to the sample, which enables direct force measurements to be performed.[22]

The force sensor was calibrated by pushing it against a hard surface, yielding the voltage-displacement sensitivity, and against a pre-calibrated AFM cantilever (NSC18-F, from MikroMasch), to obtain the spring constant of the sensor. Details about the calibration process have been given in an earlier work, where a similar instrument was calibrated.[12] The AFM instrument is fitted in a TEM specimen holder and was operated inside a JEOL (JEM

[a)] Electronic mail: henrik.jackman@kau.se

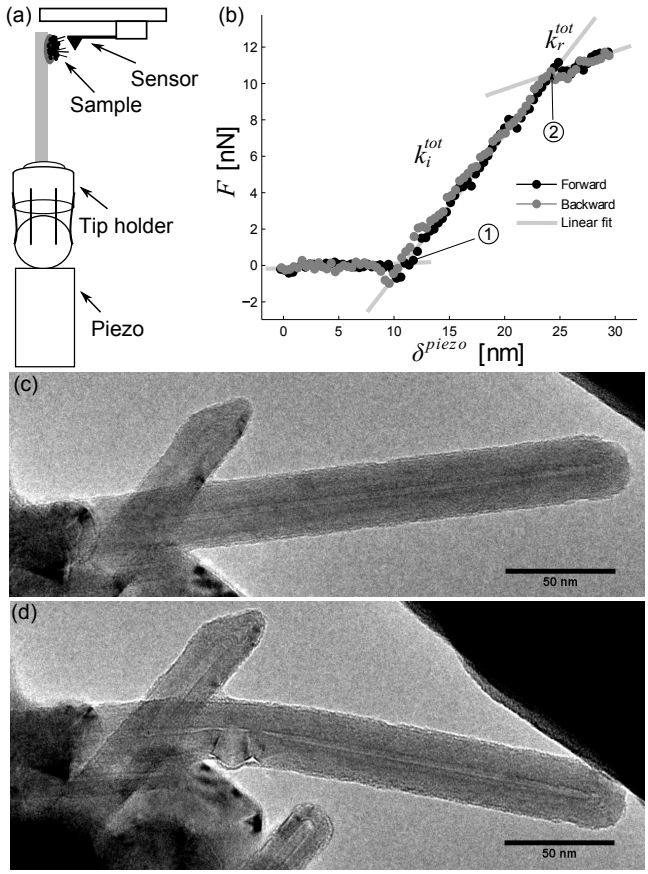

FIG. 1. (a) Experimental set-up. (b) Typical force-displacement curve from measurements on a MWCNT, where the critical displacement is defined as the distance between point 1 and 2. (c,d) TEM-images of a MWCNT, (c) undeflected and (d) deflected well past the rippling onset.

2100) TEM, equipped with a LaB_6 cathode and a digital camera from Gatan (SC1000 Orius).

The TEM was initially used to localize and to position individual CNTs in front of the force sensor. During force measurements the beam was kept away from both the sample and the sensor in order to avoid beam induced depositions and noise in the force sensor signal. After the force measurements were made, images of the CNT were acquired so that the dimensions of the CNT could be accurately determined.[20] In order to avoid beam damage of the nanotubes, an acceleration voltage of 80 kV was used during all measurements, since higher acceleration voltages are known to induce knock-on displacements of the atoms in graphene.[23] Individual CNTs were pushed against the force sensor in a cantilever to cantilever fashion, relating their spring constants to the total spring constant through:

$$k^{CNT} = \frac{k^{sens}k^{tot}}{k^{sens} - k^{tot}} \tag{1}$$

Where k^{CNT}, k^{sens}, and k^{tot} are the spring constants of the CNT, the sensor and the total spring constant, respectively. In Fig. 1 (b) a typical force-displacement curve is shown wherein at point 1 the CNT is in contact with the cantilever with zero deflection, having been deflected back after the snap-in. From this point the force increases linearly with the displacement applied to the piezo, δ^{piezo}, with spring constant k_i^{tot}. At a critical displacement, point 2, there is a kink in the force curve, where the spring constants abruptly decreases to k_r^{tot}. Upon retraction of the sample, the force-displacement curve follows a similar route as when going forward, evidence of the elastic nature of the rippling deformation. The critical displacement for the onset of rippling, δ_{cr}^{piezo}, is taken as the displacement between point 1 and 2, related to a critical displacement of the CNT through:

$$\delta_{cr}^{CNT} = \delta_{cr}^{piezo}\left(1 - \frac{k_i^{tot}}{k^{sens}}\right) \tag{2}$$

Approximating the CNTs to be cantilevered beams with a circular cross-section, the critical strain of the CNT can be calculated using:

$$\varepsilon_{cr} = \delta_{cr}^{CNT}\frac{3}{2}\frac{d_o}{l^2} \tag{3}$$

where d_o and l is the outer diameter and the length of the CNT respectively and are obtained from TEM images.[20] Using the obtained spring constant, the axial Young's modulus of the CNT can be calculated from:

$$E_z = \frac{64}{3\pi}\frac{k_i^{CNT}l^3}{(d_o^4 - d_i^4)} \tag{4}$$

where d_i is the inner diameter of the CNT. Since the spring constant used in Eq. 4 is prior to the rippling onset, the axial Young's modulus will not display any diameter dependence related to rippling effects. Such a dependence can however arise if E_z is determined from the CNT eigenfrequency, where a combination of k_i^{CNT} and k_r^{CNT} can contribute to the bending stiffness.[6,24]

TEM-images of a typical CNT are shown in Fig. 1, undeflected (c) and while deflected well past its critical displacement (d). The exact nature of the deformations appearing in the rippled phase are beyond the scope of this letter, and here we focus on the behaviour up to the critical point.

The obtained values of the critical strain for a number of tubes are plotted versus the outer diameter in Fig. 2 (a), along with values from a previous study, where ε_{cr} was measured for CVD-grown MWCNTs.[12] The values from the present study show significantly lower values of ε_{cr} at similar nanotube diameters, and are also closer to the theoretical predictions.[14,15,25]

A plot of the axial Young's modulus versus the outer diameter in Fig. 2 (b) shows that the CNTs in this study have higher values, $E_z = 780 \pm 320$ GPa, compared to the CVD-grown CNTs in the previous study.[12] We attribute this difference to a higher crystallinity in the arc-discharge grown CNTs, compared to CVD-grown ones. Modeling have shown that ε_{cr} increases with increasing

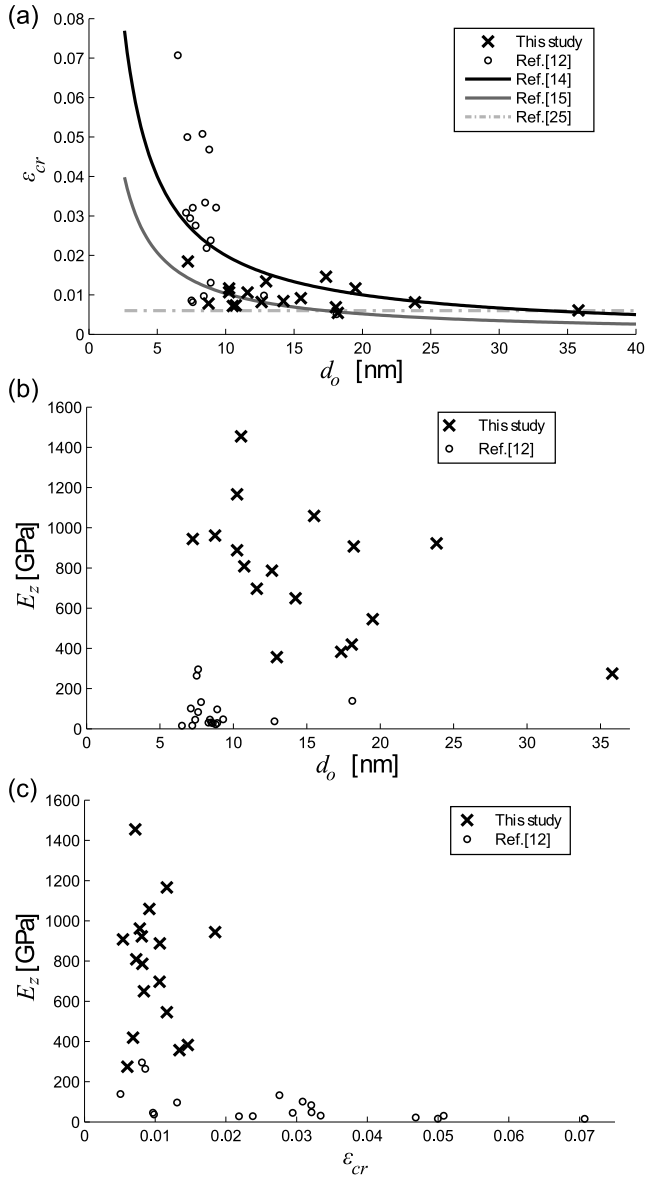

FIG. 2. (a) Measured values for the critical strain plotted versus the nanotube outer diameter, along with previous modeling. (b) Young's modulus plotted versus the outer diameter. (c) Young's modulus plotted versus the critical strain.

defect density.[26] Thereby, CNTs with a high defect density will have low E_z accompanied by high ε_{cr} values, which was indeed found for the CVD-grown nanotubes.[12] For the arc-discharge grown tubes of this study we find no such correlation, instead all tubes display high E_z and low ε_{cr} values independent of d_o, as seen in Fig. 2(c), consistent with a high crystallinity in these tubes. An early study suggested that the critical strain of single walled carbon nanotubes (SWCNTs) should depend on d_o as:[13]

$$\varepsilon_{cr} = \frac{0.077}{d_o} = \frac{0.0385}{r_o} = \frac{l_{cr}}{r_o} \tag{5}$$

A similar dependence of ε_{cr} on d_o have also been found

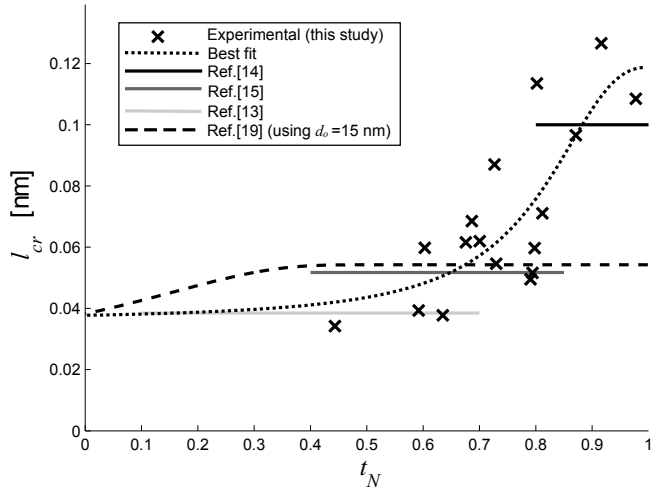

FIG. 3. Obtained values for the critical length, $l_{cr} = \varepsilon_{cr} r_o$, versus the normalized thickness t_N, together with a best fit to Eq. 7 and previous modeling results.

when modeling MWCNTs, but the suggested values of l_{cr} varies. The critical length is found to be higher for thick MWCNTs and values of $l_{cr} = 0.10$ nm and $l_{cr} = 0.052$ nm have been reported.[14,15]

Molecular mechanics simulations of the behaviour of MWCNTs under bending showed that inserting more walls in a MWCNT will increase ε_{cr}. The modeling showed small variations in l_{cr} that leveled off to a constant value after the insertion of only a few walls.[19] In order to investigate such a variation, and to compare different tubes, we define a dimensionless constant that describes a normalized thickness; $t_N = \frac{d_o - d_i}{d_o}$. In Fig. 3 the obtained critical length values, $l_{cr} = \varepsilon_{cr} r_o$, are plotted versus the normalized thickness along with different theoretical models.[13–15,19] The results from the theoretical modeling have been illustrated in the approximate t_N-region in which they were modeled. Our results show that l_{cr} varies throughout the whole range of t_N and continues to increase even for very thick MWCNTs, in contrast to the previous modeling results.[19] We attribute the increase to a supporting effect from the inner tubes, preventing the MWCNT from rippling at strains where a SWCNT, or a thin MWCNT, would already ripple or buckle.

The supporting ability of the inner tubes should depend on their radial stiffness. Treating the nanotube as a cylinder composed of a transversely isotropic material, having two in-plane Young's moduli, $E_\varphi = E_z$, a radial Young's modulus, E_r, and a Poisson's ratio, $\nu_{r\varphi}$, the normalized radial stiffness can be written as:[20]

$$S_N(t_N) = \frac{1 - (1 - t_N)^{2n}}{1 - \left(\frac{1+\nu_{r\varphi} n}{1-\nu_{r\varphi} n}\right)(1 - t_N)^{2n}} \tag{6}$$

where $n = \sqrt{\frac{E_\varphi}{E_r}}$. We have used Eq. 6 to fit the data in Fig. 3, by assuming that S_N increases the critical length

from a minimum to a maximum value as t_N varies:

$$l_{cr}(t_N) = l_{cr}^{t_N=0} + \left(l_{cr}^{t_N=1} - l_{cr}^{t_N=0}\right) S_N(t_N) \qquad (7)$$

Eq. 7 was fitted to the experimental data in Fig. 3 using the method of least squares. The best fit was found for $l_{cr}^{t_N=0} = 0.038$ nm, $l_{cr}^{t_N=1} = 0.119$ nm, $\nu_{r\varphi} = 0.79$, and $n = 1.23$ (corresponding to $E_r = 520$ GPa by using $E_\varphi = 780$ GPa). The value of $l_{cr}^{t_N=0}$ can be seen as the critical length for a CNT where $d_i \approx d_o$ and the fitted value agrees very well with the modeling results for SWCNTs.[13] The value of $l_{cr}^{t_N=1}$ then corresponds to a critical length for MWCNTs having $d_i \ll d_o$, and the fitted value is close to the modeling results for thick MWCNTs.[14] Radial Young's moduli of similar magnitude, as that obtained from the fitting, have been reported for MWCNTs,[27] although reported values of E_r vary by almost three orders of magnitude.[28] The Poisson's ratio $\nu_{r\varphi} = -\frac{\partial \varepsilon_\varphi}{\partial \varepsilon_r}$ correspond to a contraction in the φ-direction when an extension is applied in the r-direction. The value obtained from the fitting satisfies the constraints on Poisson's ratio for a transversely isotropic material ($\nu_{r\varphi}^2 < \frac{E_r}{E_\varphi}$) and similar values have been suggested from modeling.[29]

For nanotubes made of other materials than carbon, we expect Eq. 7 to be valid after appropriate adjustments of material parameters and the values of $l_{cr}^{t_N=0}$ and $l_{cr}^{t_N=1}$. The variations in the critical length will be important for applications that exploit the bending stiffness of nanotubes, such as nanoresonators[1,2] and nanorelays.[3,4] The critical displacement of a nanotube is proportional to l_{cr} and dependent on the clamping geometry.[20] In resonators using CNTs, the nanotube should be single-walled (or few-walled) and care must be taken to keep the strain within the linear region, i.e. where $\varepsilon < \varepsilon_{cr} = \frac{l_{cr}}{r_o} = \frac{0.04}{r_o}$. In relays the nanotube could well be a multiwalled one and the strain could then be increased by up to a factor three, $\varepsilon < \varepsilon_{cr} = \frac{l_{cr}}{r_o} = \frac{0.12}{r_o}$, in order to enable a larger amplitude and higher pullback force. In bi-stable relay applications one could instead exploit the lower bending stiffness of the rippled phase and use strains that are well within the rippling region.

It is worth noting that the non-stiction relays in the work of Loh et al.[17] all operate well past the critical strain for rippling, according to our findings. This lowers the restoring force of the cantilevered CNT, thus requiring an even larger relay-gap in order to avoid stiction. Although operational, both the resonance frequency and quality factor would be lower than optimum for these relays.

In conclusion, we have obtained values of the critical length in highly crystalline MWCNTs. Large variations (a factor of three) in the critical length have been observed and we attribute this to a supporting effect from inner walls in the nano-tubular structure. Based on classical material constants we provide an analytical expression for the variations of the critical length. This will provide important guidelines for the maximum deflection that can be utilized in applications such as nanoresonators and nanorelays. With appropriate adjustment of material parameters, the expression should be valid in general for concentric nano-tubular structures of different materials.

Financial support from the Swedish Research Council (project number 2010-4324) is gratefully acknowledged.

[1] V. Sazonova, Y. Yaish, H. Üstünel, D. Roundy, T. A. Arias, and P. L. McEuen, Nature **431**, 284 (2004)
[2] J. Chaste, A. Eichler, J. Moser, G. Ceballos, R. Rurali, and A. Bachtold, Nat. Nanotech. **7**, 301 (2012)
[3] J. M. Kinaret, T. Nord, and S. Viefers, Appl. Phys. Lett. **82**, 1287 (2003)
[4] S. Axelsson, E. E. B. Campbell, L. M. Jonsson, J. Kinaret, S. W. Lee, Y. W. Park, and M. Sveningsson, New J. Phys. **7**, 245 (2005)
[5] O. Lourie, D. M. Cox, and H. D. Wagner, Phys. Rev. Lett. **81**, 1638 (1998)
[6] P. Poncharal, Z. L. Wang, D. Ugarte, and W. A. de Heer, Science **283**, 1513 (1999)
[7] Y. Huang, J. Lin, M. S. Wang, K. Faerstein, C. Tang, Y. Bando, and D. Golberg, Nanoscale **5**, 4840 (2013)
[8] D. Golberg, P. M. F. J. Costa, O. Lourie, M. Mitome, X. Bai, K. Kurashima, C. Zhi, C. Tang, and Y. Bando, Nano Lett **7**, 2146 (2007)
[9] M. S. Wang, I. Kaplan-Ashiri, X. L. Wei, R. Rosentsveig, H. D. Wagner, R. Tenne, and L. M. Peng, Nano Res. **1**, 22 (2008)
[10] E. W. Bucholz and S. B. Sinnott, J. Appl. Phys. **112**, 123510 (2012)
[11] E. W. Wong, P. E. Sheehan, and C. M. Lieber, Science **277**, 1971 (1997)
[12] H. Jackman, P. Krakhmalev, and K. Svensson, Appl. Phys. Lett. **98**, 183104 (2011)
[13] B. Yakobson, C. Brabec, and J. Berhnolc, Phys. Rev. Lett. **76**, 2511 (1996)
[14] I. Arias and M. Arroyo, Phys. Rev. Lett. **100**, 085503 (2008)
[15] I. Nikiforov, D. B. Zhang, R. D. James, and T. Dumitrică, Appl. Phys. Lett. **96**, 123107 (2010)
[16] O. Loh and H. D. Espinosa, Nat. Nanotech. **7**, 283 (2012).
[17] O. Loh, X. Wei, C. Ke, J. Sullivan, and H. D. Espinosa, Small **7**, 79 (2011).
[18] C. Bower, R. Rosen, L. Jin, J. Han, and O. Zhou, Appl. Phys. Lett. **74**, 3317 (1999)
[19] T. Chang, W. Guo, and X. Guo, Phys. Rev. B **72**, 064101 (2005)
[20] See supplementary material at [URL will be inserted by AIP] for details regarding how the diameter and length were measured, a derivation of the radial stiffness, and expressions for critical displacements in two clamping geometries.
[21] Professor Hui-Ming Cheng at the Institute of Metal Research, Chinese Academy of Sciences, Shenyang, China.
[22] A. Nafari, D. Karlen, C. Rusu, K. Svensson, H. K. Olin, and P. Enoksson, J. Microelectromech. S. **17**, 328 (2008)
[23] J. C. Meyer, F. Eder, S. Kurasch, V. Skakalova, J. Kotakoski, H. J. Park, S Roth, A. Chuvilin, S. Eyhusen, G. Benner, A. V. Krasheninnikov, and U. Kaiser, Phys. Rev. Lett. **108**, 196102 (2012)
[24] J. Liu, Q. Zheng, and Q. Jiang, Phys. Rev. Lett. **86**, 4843 (2001)
[25] J. Liu, Q. Zheng, and Q. Jiang, Phys. Rev. B **67**, 075414 (2003)
[26] X. Huang and S. Zhang, Appl. Phys. Lett. **96**, 203106 (2010)
[27] I. Palaci, S. Fedrigo, H. Brune, C. Klinke, M. Chen, and E. Riedo, Phys. Rev. Lett. **94**, 175502 (2005)
[28] H. Shima, Materials **5**, 47 (2012)
[29] R. C. Batra and A. Sears, Modelling Simul. Mater. Sci. Eng. **15**, 835 (2007)